Progress In Electromagnetics Research C, Vol. 50, 1–9, 2014

A Differential K-Band UWB Transmitter for Short Range Radar Application with Continuous Running Local Oscillator

Kristian G. Kjelgård* **and Tor S. Lande**

Abstract—The design of a differential K-band UWB (Ultra Wideband) Short Range Radar (SRR) transmitter in 90 nm bulk CMOS is presented. Implementation of SRRs in deep submicron CMOS technology is attractive, in terms of cost and monolithic integration of RF font-end with signal base-band processor. The transmitted pulse bandwidth limits the range resolution of the radar system. Due to the wide bandwidth and high frequency of CMOS implementation, UWB transmitters in the K-band are challenging to make and critical for the system performance. The design presented is based on frequency up conversion using a double balanced mixer. The differential output is combined and matched with the antenna using an on-chip balun. To mitigate local oscillator (LO) leakage of UWB differential transmitters we propose a new Pulse Generator (PG) design. A switching technique is used to minimize the LO leakage enabling continuous wave operation with very wideband pulses. Measurements of the proposed transmitter achieves a −10 dB bandwidth (BW) of 5 GHz. Using a Pulse Repetition Frequency (PRF) of 100 MHz the peak average power is −40 dBm. Compared to measured transmitter performance of a single balanced mixer design, the LO leakage of this dual balanced mixer is decreased with more than 20 dB, and is lower than the peak average power of the pulse. It consumes 11 mW from a 1.2 V supply where 6 mW is from the LO.

1. INTRODUCTION

Paramount in car safety today is driver assisting technology and human protection systems. Modern high-end cars have several advanced systems assisting the driver. Typical driver assist devices are video cameras for lane departure warning and vision aid during reversing, ultra sound parking sensors and radar for adaptive cruise control and collision mitigation. For future improvement of safety, like blind-spot detection, parking-assist, adaptive cruise control and collision warning are predicted to be important [1]. The success criteria for implementation of these systems are low cost, high range resolution and large detection range [1]. After the FCC and ETSI opened the K-band (22–29 GHz) for ultra wideband automotive radar application, an increased research activity on the design and implementation of radar systems have emerged [2–6]. The main focus is toward K-band front-end circuits in CMOS. With very high $f_t/f_{\max}$ and low cost, deep sub-micron CMOS technology make single chip radar systems feasible. The implementation of K-band SRR systems in CMOS are challenging due to the very wide bandwidth at near millimeter wave frequencies. With an available bandwidth of 7 GHz optimal RF front-end design is very challenging and critical for the overall system performance [7].

In Figure 1, the proposed system architecture for a full system implementation is illustrated. The frequency range is extended to the K-band with a direct conversion front-end. The core processor provides a digital trigger signal to the PG, which generate a pseudo-Gaussian pulse. The pulse is multiplied with the LO in the mixer and transmitted at the target. The received pulse is then amplified in a LNA, down-converted and processed. This paper focuses on the design of the transmitter (TX), as

Received 21 March 2014, Accepted 27 April 2014, Scheduled 30 April 2014
* Corresponding author: Kristian G. Kjelgård (kristigk@ifi.uio.no).
The authors are with the Department of Informatics, University of Oslo, Norway.

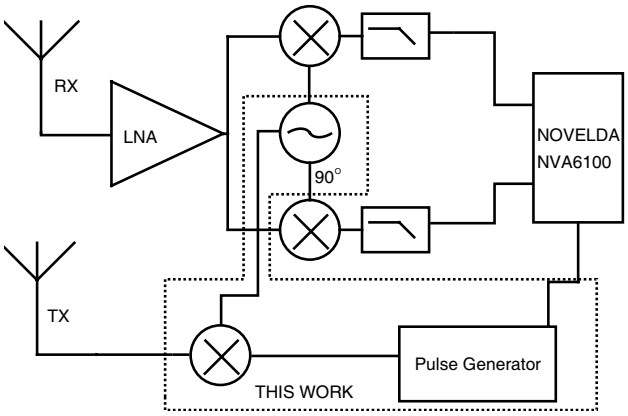

Figure 1. System architecture.

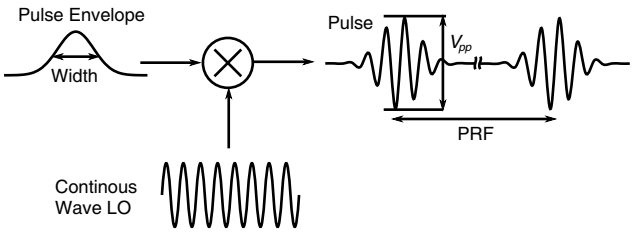

Figure 2. Transmitter operation.

marked in Figure 1. The TX is a critical part of the radar system. To fully utilize the available frequency spectrum and maximize the overall system resolution it is important to maximize the bandwidth of the transmitted pulses. However, the average and peak transmitting power must comply with the regulations. The maximum average power is limited to $-41.3\,\mathrm{dBm/MHz}$ in a 7 GHz window and $-61.3\,\mathrm{dBm/MHz}$ outside (FCC).

In Figure 2 the ideal up-conversion mixing of a Gaussian shaped sine wave is shown. The pulse-shape, center frequency and peak-to-peak voltage (V_{pp}) of the pulses determine the shape of frequency spectrum. Together with the Pulse Repetition Frequency (PRF) the average power spectrum of the transmitter is defined. The peak power limitation is $0\,\mathrm{dBm}/50\,\mathrm{MHz}$, and for systems with a high PRF, the average power limitation will be exceeded before the peak power limitation. The signal processor in the proposed system architecture supports staggered PRF and at 100 MHz the unambiguous range is still 60 m. The transmitter considered in this paper is implemented in standard CMOS technology to allow monolithic integration with the NVA6100 signal processor [8, 9].

In literature, several works on CMOS K-band UWB transmitters for short range radars have been presented [3, 4, 6, 10–12]. Seen in [11] and other works, LO based transmitters are prone to Local Oscillator (LO) leakage. In [3, 4, 6] the oscillator is pulsed to mitigate LO leakage and save power. However, for a fully integrated transceiver with shared LO, continuous operation of the LO is required by the receiver. As observed in previous generation of this transmitter [11], based on a single-balanced mixer, the Local Oscillator (LO) leakage is in violation of the regulations. Here the LO is coupled to the output through the gate-drain capacitance of the mixer transistors.

To reduce the LO leakage and power consumption we propose to implement the transmitter with a double-balanced mixer and a differential Pulse Generator (PG). Reducing LO-leakage with double-balanced mixers is well known design technique, however with a 5 GHz bandwidth Gaussian pulse envelope implementation of differential PG is not trivial due to the nature of the pulse shape. A PG with inverted output is presented in [6]. Here the PG directly drives a variable attenuators at a differential RF output shaping the LO signal. The output attenuators is not efficient enough for LO leakage isolation and there is still $-26\,\mathrm{dBm}$ of LO at the output. This is mitigated with pulsing the LO.

For double-balanced mixers a true differential PG is required. To set the common-mode voltage of the differential pulse a high pass filter is inserted in the signal path. Due to the wide bandwidth of the pulse, a very low cut-off frequency is required to avoid pulse shape distortion. However, too low cutoff frequency result in accumulation of a differential voltage offset after the filter giving severe LO leakage. By using reset switches in the DC-block filter and effectively changing the RC time constant of the filter after each pulse, the offset voltage the LO leakage of differential pulse-generator is minimized.

The design is presented in Section 2. For comparison, measurement results of both a single-ended and differential transmitter is presented in Section 3. All the simulations and measurements are from chips made in a 90 nm bulk CMOS process with a $f_t/f_{\max}$ frequency over 100 GHz, supply voltage of 1.2 V and substrate resistivity of $\approx 10\,\Omega/\mathrm{cm}$.

2. CIRCUIT DESIGN

The transmitter includes an edge-triggered differential pulse generator, double-balanced mixer and a lumped Marchand type balun. Schematic of the transmitter is shown in Figure 3. After a trigger edge the pulse generator outputs a differential pulses to the mixer to be up-converted with the LO frequency. The balun effectively match the impedance of the TX differential output and combines the signal to the antenna.

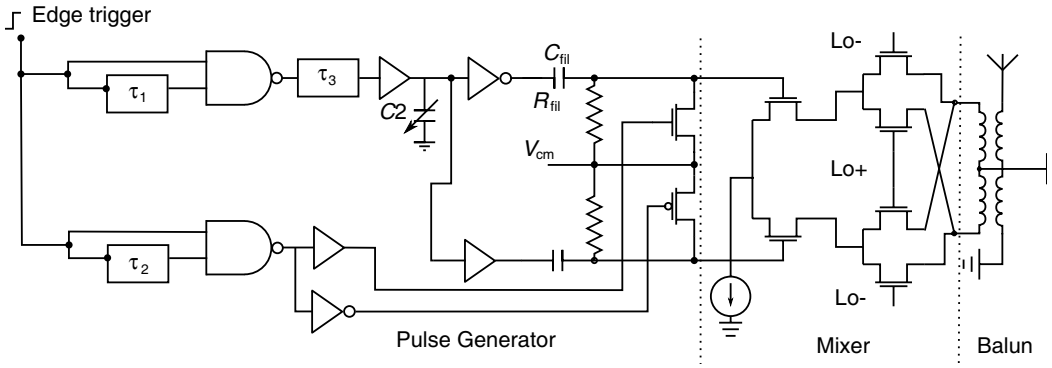

Figure 3. Circuit schematic.

2.1. Pulse Generator

The pulse generator outputs the pulse envelope to the mixer and the pulse shape defines the bandwidth and frequency spectrum of the transmitted pulse. To minimize the side-lobe levels in the frequency domain, a Gaussian pulse-shape in the time-domain is the optimal pulse shape. The PG mimics the Gaussian shape by utilizing the non-linear characteristics of the CMOS inverter. The single ended PG is shown in Figure 4. The capacitor, $C1$, is used to tune the pulse width $\Delta\tau$ and $C2$ is loading the buffer limiting the slope of the pulse. With a triangular pulse (T) as the input of a current starved inverter, the output pulse (P) shape is sufficiently close to a Gaussian [11].

As proposed, to reduce the LO-leakage of the transmitter, the mixer can be implemented as a double-balanced Gilbert mixer. This effectively cancels the LO leakage due to the gate-drain capacitive coupling. However, a double-Balanced mixer requires a differential pulse signal. And if any differential offset is present at the pulse input, LO leakage will occur at the output.

A schematic of the differential pulse generator is shown in Figure 5. Both a buffer and an inverter is now driven by the triangular pulse, with the result of two inverted pseudo-Gaussian pulses. For a

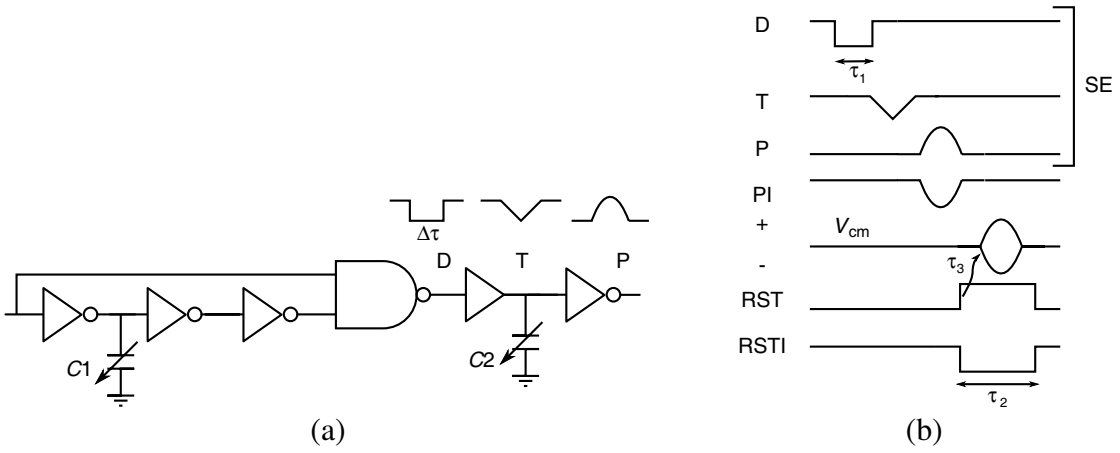

Figure 4. Pulse generation. (a) Single-ended PG. (b) Pulse event diagram SE/DIFF.

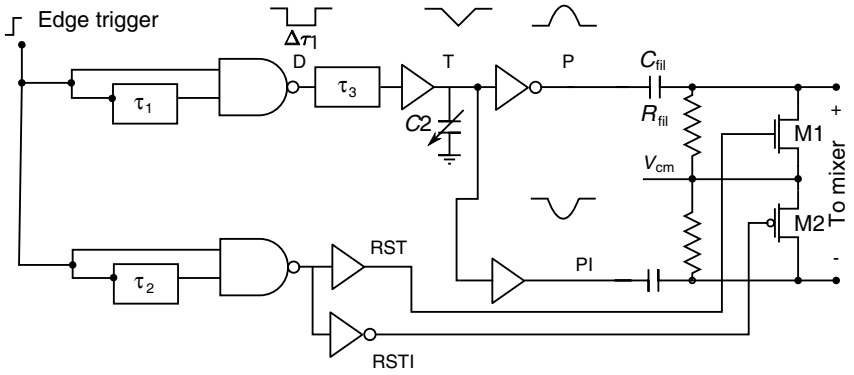

Figure 5. Differential pulse generator.

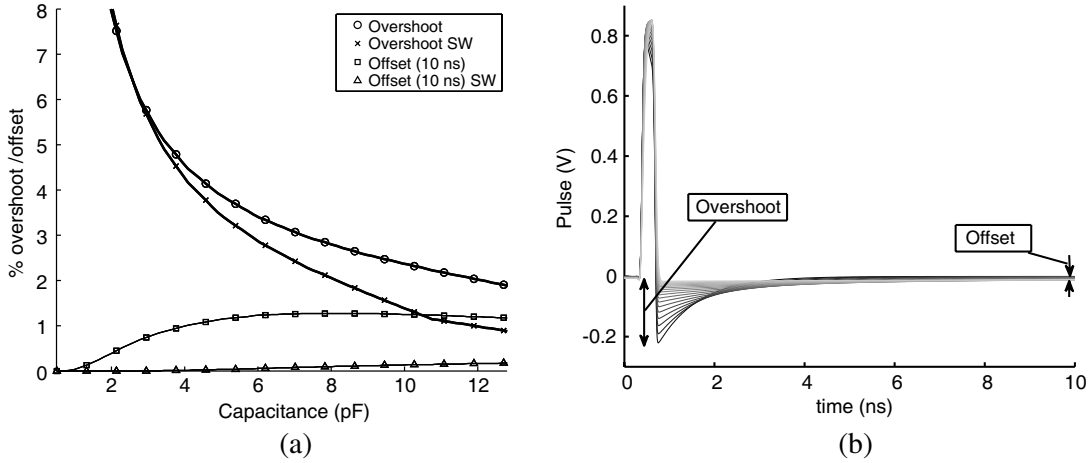

Figure 6. Simulation of pulse distortion. (a) Percent overshoot and offset simulation. (b) Family transient simulation.

differential pulse, the DC level of the inverted pulses is combined to establish a common mode voltage. This common mode voltage is also used to bias the RF transistors of the mixer. To set the common-mode voltage DC-blocking, high-pass RC filters are inserted in the signal path. The common mode voltage is set at the V_{cm} node, as shown in Figure 5.

For shaping of the UWB pulses the time-constant of the RC filter must be carefully chosen. If the time-constant of the RC filter is on the same order as the pulse length, the pulse will be distorted. And when the time-constant of the RC filter is much larger than the pulse-length the differential voltage is not efficiently set to zero after each pulse. In Figure 6(b) the transient response of the positive pulse output is illustrated. The filter capacitor C_{fil} is ranging from 2 to 13 pF with a fixed resistance R_{fil} of 1.37 kΩ. As a qualitative measure of the pulse distortion we use the percent overshoot. The offset $(V_+ - V_{CM})$ at 9 ns after the pulse is used as measure of how efficiently the pulse is reset.

To mitigate this effect we propose to reset the differential voltage to zero after each pulse. A switch control pulse is generated, and transistors M1/2 are turned on when not transmitting. To minimize the capacitive loading of the signal path, the NMOS transistor is connected to the + and the PMOS to the − wire. With the signal at a higher voltage than the common mode voltage for the NMOS and lower for the PMOS, source terminal of the transistors are loading the signal path, minimizing the parasitic capacitance.

In Figure 6(a) simulations of the overshoot and offset as a function of the capacitance is show. And as expected, the offset after 9 ns is significantly reduced with the reset switches. The overshoot voltage is also reduced for capacitance values larger than 3 pF as the reset is enabled before the previous minimum voltage.

2.2. VCO, Mixer & Balun

The differential pseudo Gaussian pulses are shifted in frequency from base band to the K-band center frequency using a double balanced Gilbert mixer. The LO signal is generated on-chip using a LC tank VCO with a MOS varactor for frequency tuning. Schematic of the mixer and LO is shown in Figure 7.

To provide a single ended output and matching for the antenna, the mixer is loaded with a balun. The balun is designed using the lumped Marchand design procedure as presented in [12, 13]. A schematic model of the balun is shown in Figure 8(b). C_c is the coupling capacitance between the balanced and unbalanced side of the balun, Lb and Lu is the inductance and C_{sb} is the substrate capacitance. To have phase balance in the balun we must have $S_{21} = -S_{31}$. By using the odd-even mode analysis of the schematic in Figure 8(a) the phase imbalance is given by Equation (1).

$$\frac{S_{31}}{S_{21}} = -\frac{Z_{0e} - Z_{0o}}{Z_{0e} + Z_{0o}} \tag{1}$$

As seen in [12], to minimize the phase imbalance the even mode impedance must be much larger than the odd mode impedance, where

$$Z_{0e} = \sqrt{\frac{L(1+k)}{C_{sb}}}, \quad Z_{0o} \simeq \sqrt{\frac{L(1-k)}{C_c + C_{sb}}} \tag{2}$$

Given the inductance of $Ls \approx Lb$, we must have $\frac{C_c}{C_{sb}} \gg 1$. The matching of the ports in the balun must also be considered, and as the capacitance seen at the drain of the mixer LO transistors effectively adds

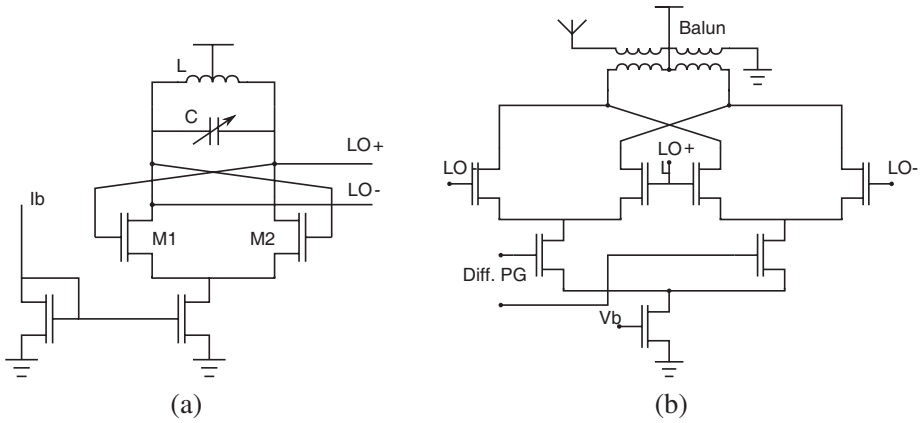

Figure 7. Frequency conversion. (a) LC VCO. (b) Double-balanced Gilbert mixer with balun.

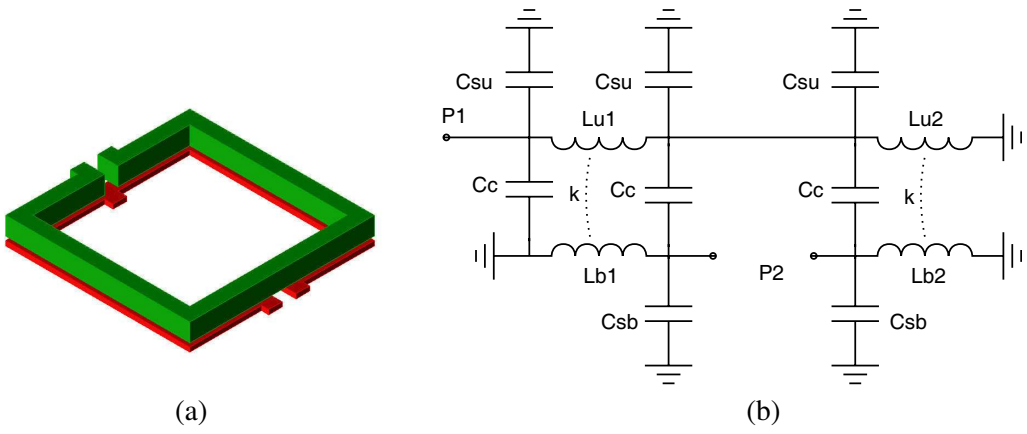

Figure 8. Lumped Marchand balun. (a) 3D animation. (b) Schematic.

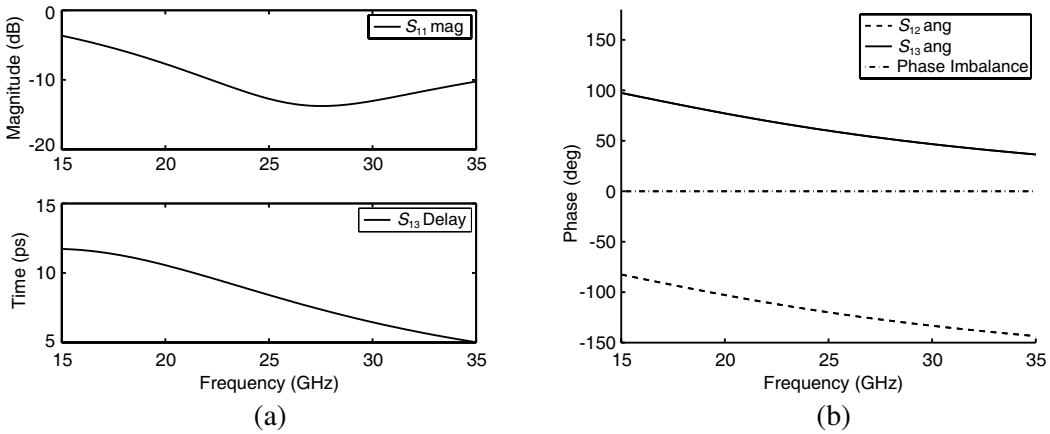

Figure 9. MOM simulations balun. (a) S_{11} magnitude and delay. (b) Phase imbalance.

to the C_{sb}, we must compensate by increasing the inductance Lb. To optimize and verify the design a parametrized layout of the balun was simulated in a 2.5-D method of moments EM simulator. To match the 50 Ω impedance of the antenna with the mixer output we used the simulated mixer output impedance as the port impedance in the MOM simulations ($10 - j25\,\Omega$).

In Figure 9 MOM simulation of S_{11}, delay and phase imbalance for a single-turn 100 µm × 100 µm balun with is shown. With low phase-imbalance, low loss and wide bandwidth this balun is suitable for this application. The layout is shown in Figure 8(a).

3. MEASUREMENTS

The test chip was implemented in TSMC 90 nm CMOS. Photo of the chip and test fixture is shown in Figure 10. The transmitter (TX) is measured with 50 Ω 100 µm pitch GSG RF wafer probes. The instruments are calibrated at the test port and the probe/cable loss is not de-embedded. At 20–30 GHz the probe/cable loss is 1.5–2 dB. Trigger signal, power and bias are provided via the PCB. The time-domain data is measured with a 80 GS/s oscilloscope and is referenced as the waveform and the FFT is post-processing of the time domain data. Measurements with the 26 GHz spectrum analyzer is referenced as the spectrum.

In Figure 11 measurements of the single ended TX previously presented in [11] is shown. The LO leakage at 26.5 GHz is clearly violating the −41.3 dB/MHz limit. The V_{pp} is 218 mV with a 5 GHz–10 dB bandwidth. At a PRF of 80 MHz and an equivalent resolution bandwidth (RBW) of 1 MHz the maximum average power is −46 dBm.

The measurements of the differential TX is shown in Figure 12. V_{ppr} is the maximum peak to peak

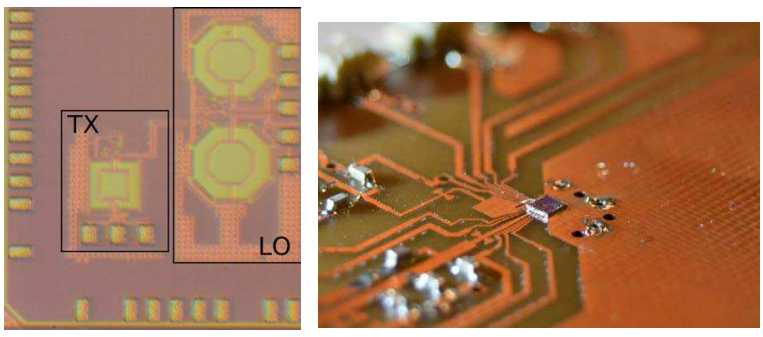

Figure 10. Prototype photography. (a) Chip photo. (b) Test fixture.

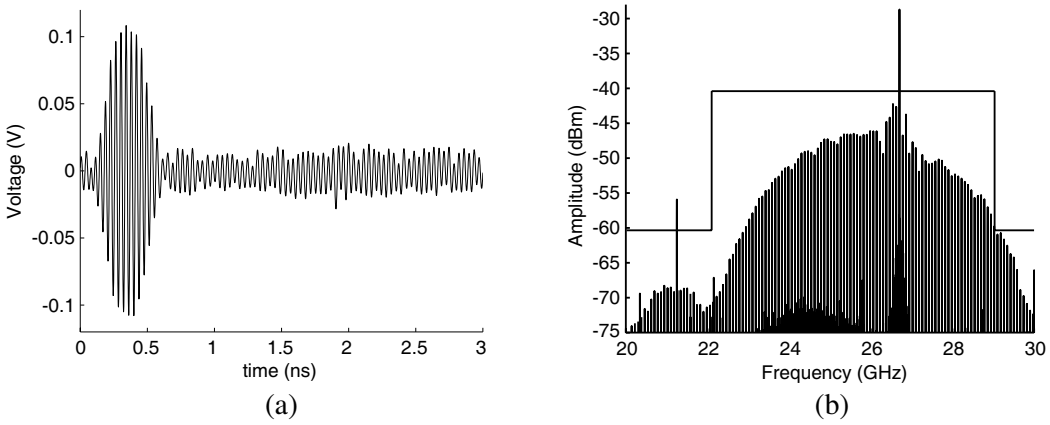

Figure 11. Measurement single ended two coil transmitter, from [11]. (a) Waveform. (b) FFT.

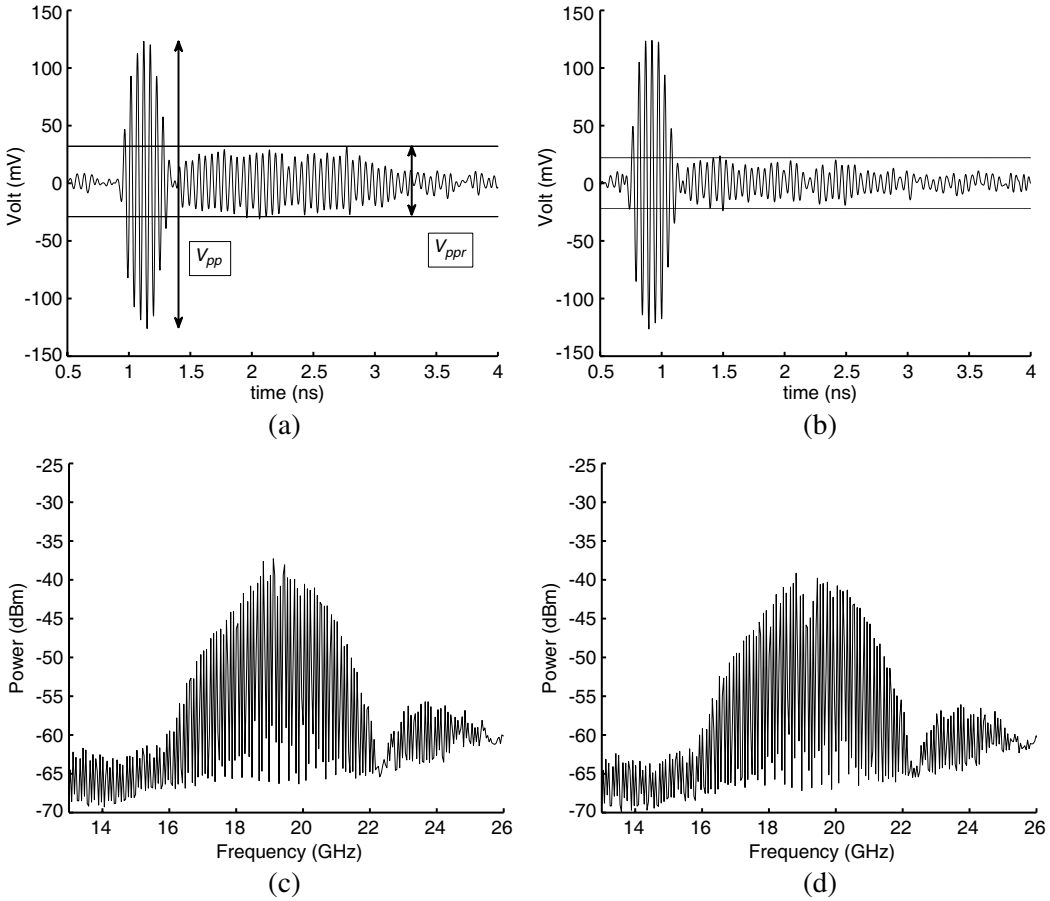

Figure 12. Measurement differential single coil balun transmitter. (a) Waveform switch off. (b) Waveform switch on. (c) Spectrum switch off. (d) Spectrum switch on.

voltage within 2 ns after the pulse. With the reset disabled V_{pp} is 250 mV and V_{ppr} 61 mV. Enabling the reset and the V_{ppr} is reduced to 44 mV while the V_{pp} remain the same. The length of the residual pulse 'tail' voltage is also suppressed resulting in a significant reduction of the LO leakage. The spectrum is shown in Figures 12(c) and 12(d) with reset switching off and on, respectively. The LO power is suppressed 6–7 dB. When the switching are enabled the time constant of the filter is decreased directly

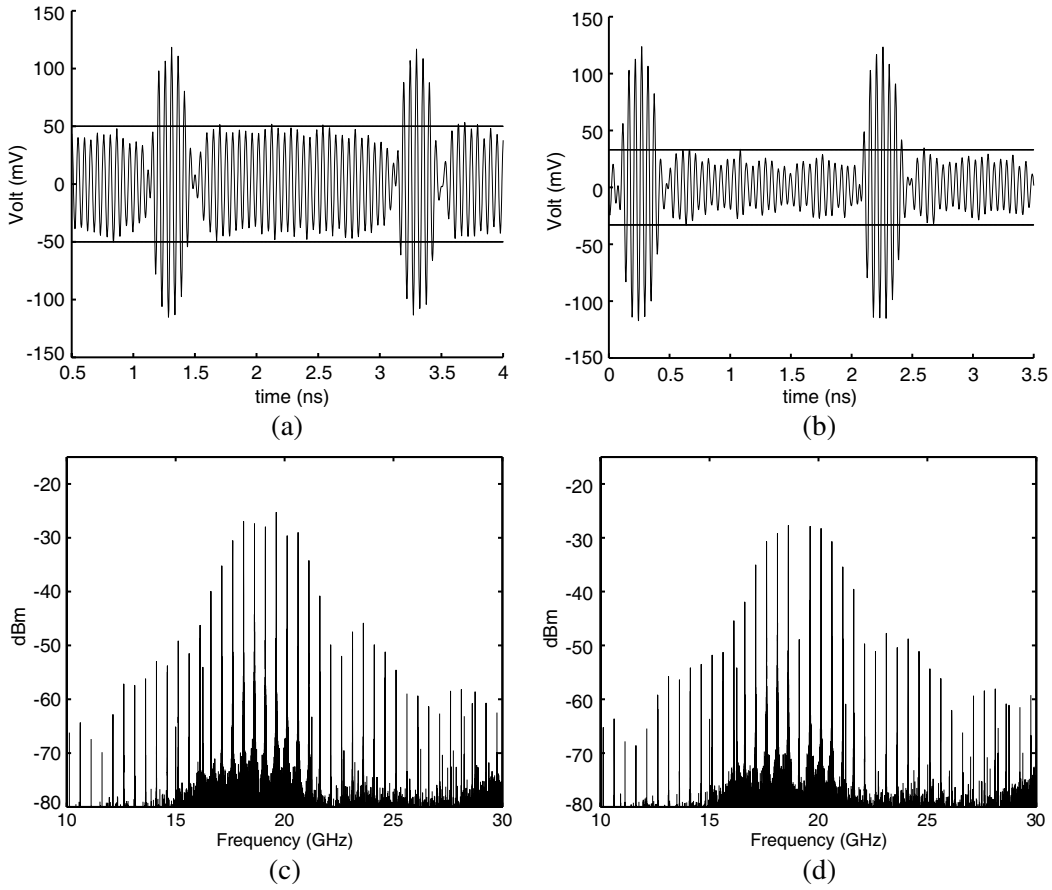

Figure 13. Measurement differential transmitter PRF = 500 MHz. (a) Waveform switch off. (b) Waveform switch on. (c) FFT switch off. (d) FFT switch on.

Table 1. Comparison of K-band IR-UWB transmitters.

	$V_{p\text{-}p}$ (mW)	BW − 10 dB (GHz)	Size (mm^2)	Arch.	Peak[1] (dBm @ MHz)	Power (mW)	LO leak (dBm)
[10]	71	3	0.004	Edge Comb	−61@	1.4	-
[2, 3]	394	3.6[2]	0.44	Pulsed LC	−55@5		-
[6]	240	4.9	0.41	Pulsed LC	-	2.2	-
[4]	430	2[3]	1.44[4]	LC+mix	−41@30	63	−59
[11] (SE)	230	5	0.3	LC+mix	−43@80	11	−28
this	260	5	0.34	LC+mix	−40@80	14 (QVCO 9)	−47

[1] w/o LO leak (@PRF) [2] BW data not available $\frac{1}{280\,\text{ps}} \approx 3.6\,\text{GHz}$ [3] 4 GHz in compressed mode

after the pulse, forcing the differential signal to zero. There is still some LO leakage due to mismatch of the mixer transistors, but well under the maximum allowed by the regulations. At higher PRF the effect is even more pronounced. When the settling time of the filer is in the order of the PRF a offset are accumulated between pulses.

In Figure 13 measurements of the transmitter operating at a PRF of 500 MHz is shown. The LO leakage is severe with a V_{ppr} of 100 mV. With switching enabled the V_{ppr} max is reduced to 60 mV and the LO is reduced with over 10 dB.

In Table 1 a comparison with state-of-the-art is presented. With a 5 GHz–10 dB BW, 6.8 GHz–20 dB BW and LO leakage less than the peak average power, the transmitter fill the regulation mask well and have the widest BW compared to prior art.

4. CONCLUSIONS

This paper proposes a CMOS UWB transmitter design based on differential PG and double balanced mixer. Compared with the single-ended PG with single-balanced mixer presented in [11], the LO leakage is significantly reduced. The new differential PG with switching of the DC-block filter time constant effectively reducing LO leakage. With a bandwidth of 5 GHz, side-lobe levels under −20 dB and low LO leakage, this transmitter is suitable for high range-resolution pulsed short-range radar. Compared with prior art we show the widest bandwidth with low LO leakage for continuous wave operation. Integration with receiver and single LO in now feasible allowing coherent operation of the radar. A single LO reduce power consumption and die area for the radar system.

REFERENCES

1. Murad, M., J. Nickolaou, G. Raz, J. S. Colburn, and K. Geary, "Next generation short range radar (SRR) for automotive applications," *IEEE Radar Conference (RADAR)*, 0214–0219, May 2012.
2. Lee, S., S. Kong, C.-Y. Kim, and S. Hong, "A low-power K-band CMOS UWB radar transceiver IC for short range detection," *IEEE Radio Frequency Integrated Circuits Symposium (RFIC)*, 503–506, Jun. 2012.
3. Lee, S., C.-Y. Kim, and S. Hong, "A K-band CMOS UWB radar transmitter with a bi-phase modulating pulsed oscillator," *IEEE Transactions on Microwave Theory and Techniques*, Vol. 60, No. 5, 1405–1412, May 2012.
4. Yang, J., G. Pyo, C.-Y. Kim, and S. Hong, "A 24-GHz CMOS UWB radar transmitter with compressed pulses," *IEEE Transactions on Microwave Theory and Techniques*, Vol. 60, No. 4, 1117–1125, Apr. 2012.
5. Jain, V., S. Sundararaman, and P. Heydari, "A 22–29 GHz UWB pulse-radar receiver front-end in 0.18-µm CMOS," *IEEE Transactions on Microwave Theory and Techniques*, Vol. 57, No. 8, 1903–1914, Aug. 2009.
6. El-Gabaly, A. M. and C. E. Saavedra, "A quadrature pulse generator for short-range UWB vehicular radar applications using a pulsed oscillator and a variable attenuator," *IEEE Transactions on Circuits and Systems I: Regular Papers*, Vol. 58, No. 10, 2285–2295, 2011.
7. Taylor, J. D., *Ultrawideband Radar: Applications and Design*, Chapter 11, CRC Press, 2012.
8. Hjortland, H. A. and T. S. Lande, "CTBV integrated impulse radio design for biomedical applications," *IEEE Transactions on Biomedical Circuits and Systems*, Vol. 3, No. 2, 79–88, Apr. 2009.
9. *Novelda Impulse Radar*, http://www.novelda.no.
10. Oncu, A., B. B. M. Wasanthamala Badalawa, and M. Fujishima, "22–29 GHz ultra-wideband CMOS pulse generator for short-range radar applications," *IEEE Journal of Solid-State Circuits*, Vol. 42, No. 7, 1464–1471, Jul. 2007.
11. Kjelgard, K. G. and T. S. Lande, "A 26 GHz UWB CMOS IR-UWB transmitter with on-chip balun," *NORCHIP*, 1–4, Nov. 2012.
12. Kjelgard, K. G. and T. S. Lande, "Design of 26 GHz UWB CMOS pulse-mode transmitter with on-chip balun for SRR applications," *2012 IEEE International Conference on Ultra-Wideband (ICUWB)*, Sep. 2012.
13. Johansen, T. and V. Krozer, "Analysis and design of lumped element marchand baluns," *17th International Conference on Microwaves, Radar and Wireless Communications, 2008, MIKON 2008*, 1–4, May 2008.